

---

# Using tracer tests and hydrological observations to evaluate effects of tunnel drainage on groundwater and surface waters in the Northern Apennines (Italy)

Valentina Vincenzi · Alessandro Gargini ·  
Nico Goldscheider

**Abstract** The impact of a railway tunnel on groundwater and surface waters in the Northern Apennines (Italy) was demonstrated and characterised by multi-tracer tests and hydrological observations. The 15-km-long Firenzuola tunnel crosses turbidite marls and sandstones previously not considered as aquifers. During the drilling, water inrushes occurred at fracture zones, and the tunnel still continues to drain the aquifer. The water table dropped below the level of the valleys, and gaining streams transformed into losing streams or ran completely dry, as did many springs, causing severe damage to the aquatic fauna and other elements of the ecosystem. Two multi-tracer tests, each using uranine and sulforhodamine G, were carried out in two impacted catchments in order to confirm and quantify the stream–aquifer–tunnel interrelations. The results proved connection between losing streams and numerous water inlets in the tunnel, with maximum linear distances of 1.4 km and velocities up to 135 m/d. Several of the demonstrated flowpaths pass under previous groundwater divides (mountain ridges), proving that the tunnel has completely modified the regional flow system. Water balance estimations demonstrate that the observed water

losses cannot be explained by climate change but can largely be attributed to the tunnel drainage.

**Keywords** Tracer tests · Draining tunnel · Hydrogeological impact · Fractured rocks · Italy

## Introduction

Hydrogeological studies related to tunnels often focus on one or several of the following aspects:

1. From a technical point of view, groundwater is a problem for the construction of tunnels.
2. From an ecological and hydrological point of view, tunnels represent a risk for groundwater and the connected surface waters and ecosystems.
3. From a scientific point of view, tunnels offer the opportunity to access and study underground environments, including aquifers and groundwater.

Many hydrogeological and engineering studies mainly deal with the first aspect. Groundwater inrushes into tunnels imply a risk for the workmen and machines, especially if these inrushes occur unexpectedly and at high pressures and/or flow rates. Groundwater can also lower the stability of the tunnel face and increase the construction time and costs (Cesano et al. 2000; Day 2004; Lee et al. 2003), or even cause collapse (Tseng et al. 2001).

Tunnels in the unsaturated zone and in low-permeability geological formations such as poorly fractured crystalline rocks, are often built as draining tunnels. Tunnels that cross the saturated zone of an aquifer, as well as tunnels below rivers or the sea, generally require impermeable linings, which entail higher technical efforts and costs (Atkinson and Mair 1983). Drainage tunnels below the groundwater level create an elongated zone of depression. The drawdown and the lateral extent of this depression depend on the depth of the tunnel below the initial water table and on aquifer hydraulic characteristics. A wide range of methods has been proposed to predict both groundwater inflow to tunnels and the drawdown

---

Received: 21 January 2008 / Accepted: 17 September 2008

© Springer-Verlag 2008

---

A preliminary version of the study has been presented, as oral communication, at the XXXV IAH Congress “Groundwater & Ecosystems” held in Lisbon on 17–21 September 2007.

---

V. Vincenzi (✉) · A. Gargini  
Earth Sciences Department,  
University of Ferrara,  
Via Saragat 1, B building, 44100, Ferrara, Italy  
e-mail: vncvnt@unife.it  
Tel.: +39-0532-974691  
Fax: +39-0532-974767

N. Goldscheider  
Centre of Hydrogeology,  
University of Neuchâtel,  
Rue Emile-Argand 11, 2009, Neuchâtel, Switzerland

caused by the tunnel such as analytical solutions for different hydrogeological settings (Goodman et al. 1965; Kolymbas and Wagner 2007; Marechal and Perrochet 2003; Perrochet 2005), including solutions for transient flow towards tunnels drilled into heterogeneous formations (Perrochet and Dematteis 2007) or tunnels in multi-layer aquifer systems (Yang and Yeh 2007), as well as different numerical models (Molinerio et al. 2002; Feinstein et al. 2003; Yoo 2005).

Any groundwater drawdown alters the natural hydrogeological flow system and can consequently impact groundwater-dependent vegetation, surface streams, lakes, wetlands and the associated aquatic ecosystems, but also springs and wells. Obviously, this can also affect the regional population and create problems related to drinking water supply, agriculture, irrigation, fishing, tourism and other activities (Sjolander-Lindqvist 2005). The magnitude of the impact depends on the drawdown and on the flow rate that is diverted from the natural system into the tunnel (Li and Kagami 1997; Kitterod et al. 2000).

The wise approach is to assess the potential hydrological and ecological impact of a tunnel before building it, and take appropriate measures to minimise the impact such as impermeable linings, at least in the sectors of the tunnel that cross the most permeable zones and/or the zones where surface waters and ecosystems are most vulnerable to groundwater drawdown (Kvaerner and Klove 2006).

The study presented in this paper deals with an example where this was not done. Between 1996 and 2005, nine tunnels with a total length of 73 km were drilled across the Northern Apennine chain, Italy, for the high-speed railway connection between Bologna and Florence. The region consists of turbidite formations including marls and sandstones that were erroneously not considered as relevant aquifers. Therefore, the tunnels were built without impermeable linings. Huge water inrushes, often from fractures and localised in specific sectors, occurred during the drilling process, and the tunnels still continue to drain the aquifer. As a result, many streams and springs in the region run partly or completely dry, obviously causing severe damage to the aquatic ecosystem, particularly the invertebrate, amphibians and fish fauna, although this impact has not been systematically monitored.

Detailed spring and surface water monitoring, along with geological and hydrogeological observations, made it possible to document the impact of the tunnel on groundwater and surface waters, and to set up a conceptual model of the tunnel–aquifer–surface interactions. It was possible to infer that the tunnels have entirely altered the natural flow systems: gaining streams transformed into losing streams, previous drainage divides lost their function, and the entire natural drainage system was replaced by underground drainage towards the tunnel (Gargini et al. 2008).

However, due to a shortage of groundwater observation wells and detailed, long-term information concerning the pre-construction state, at some places this conceptual model was lacking solid evidence. Although the impact

of the tunnel seemed obvious, it was difficult to prove that the alteration of the natural drainage system was not, for example, due to climate change. Therefore, starting from the results of Gargini et al. (2008), a new study was performed during years 2005–2007, after the tunnel completion, with new specific field measurements and investigations on the impacted streams, new tunnel surveys and several tracer tests between the losing surface streams and the tunnels.

This paper presents the results of this study at the Firenzuola tunnel, where the most severe impacts have been observed and studied in several catchments. The main goals were:

1. To confirm (or refute) the conceptual model of regional groundwater and surface waters drainage by the tunnel, even across previous drainage divides
2. To characterise the impact on streams waters, in relation to geological features, in order to evaluate possible mitigation measures for the maintenance of a minimum summer flow
3. To better characterise and quantify the flow paths, flow velocities, flow rates and flow processes in this anthropogenically altered hydrogeological system
4. To obtain insights into the hydrogeology of turbidite formations
5. To test the applicability of artificial tracers for this type of problem and hydrogeological setting

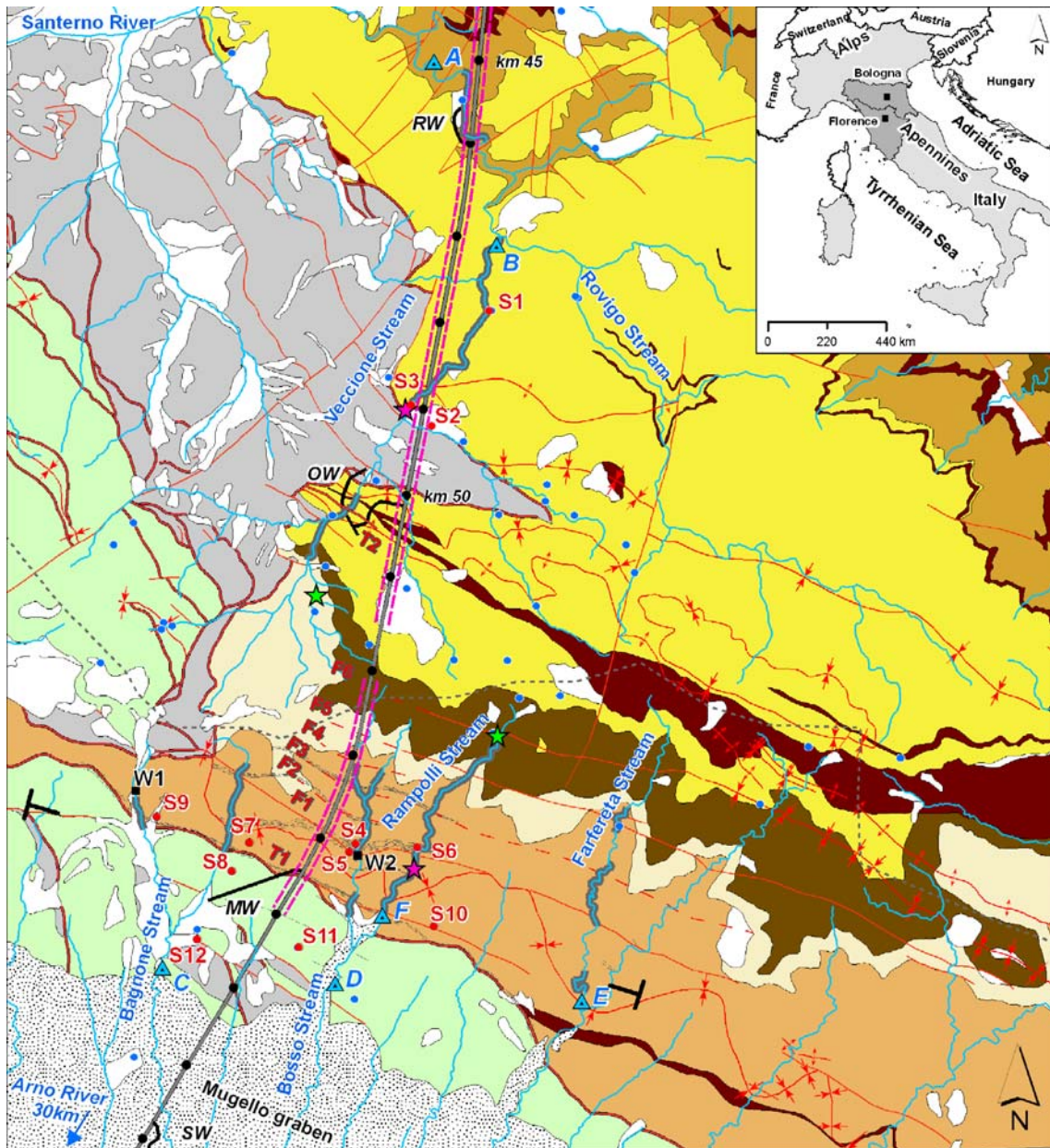
## Description of the study area

### General geological and hydrogeological setting

The Firenzuola tunnel is 15,060 m long and crosses the main Apenninic water divide between Santerno River to the north and Arno River to the south (Fig. 1). Drilling began in 1996 through four access windows (total length: 3,519 m) and was completed at the end of 2005.

The tunnel is mostly drilled through silico-clastic turbidite units of the Miocene Marnoso Arenacea Formation (MAF), consisting of arenitic layers (sandstones) and pelitic layers (marls; Ricci Lucchi 1986; Zattin et al. 2000). The MAF can be subdivided into lithostratigraphic members according to the ratio of arenitic to pelitic layers (A/P ratio) (Cibin et al. 2004; Gargini et al. 2006; Amy and Talling 2006). The tunnel crosses two members with high A/P ratios (i.e. predominantly sandstones): Nespole member, from the kilometric progressive (p.) 48+000 km to p. 49+500 km, and Premilcuore member, from p. 51+600 km to p. 54+700 km (Fig. 1).

The Apenninic chain is a typical thrust-fold belt resulting from compression tectonics, followed by a post-orogenic extension phase in its southern part. Firenzuola tunnel is located at the border between two different tectonic domains: the first one (north of the main water divide) has been subjected to a dominant compressive tectonic stress field; the second one (farther to the south) has been subjected to an extensional tectonic phase



### Legend

<ul style="list-style-type: none"> <li>— Firenzuola Railway Tunnel</li> <li>— Access windows (RW,OW,MW,SW)</li> <li>• Progressive (every km)</li> <li>--- Topographic divide</li> <li>• Main spring (not impacted)</li> <li>— Main stream (not impacted)</li> <li>▲ Stream section</li> <li>⊥ Section of conceptual model (Fig. 2)</li> </ul>	<p><b>TURBIDITES</b></p> <ul style="list-style-type: none"> <li>■ Tuscan Unit turbidites</li> </ul> <p><b>MAF members</b></p> <ul style="list-style-type: none"> <li>■ Nespoli m. (A/P&gt;1)</li> <li>■ Bassana m. (A/P=1)</li> <li>■ Galeata m. (A/P=0.3)</li> <li>■ Premilcuore m. (A/P&gt;1)</li> <li>■ Olistostromes</li> <li>■ Argillitic and marly m.</li> </ul>	<ul style="list-style-type: none"> <li>□ Landslides / alluvial deposits</li> <li>▨ Fluvio-lacustrine deposits</li> <li>▨ Argillitic and marly units</li> </ul> <p><b>TECTONIC FEATURES</b></p> <ul style="list-style-type: none"> <li>— Fault</li> <li>— Thrust</li> <li>— Anticline</li> <li>— Syncline</li> <li>— Fractured zone</li> </ul>	<p><b>IMPACTS</b></p> <ul style="list-style-type: none"> <li>■ on well</li> <li>• on spring</li> <li>— on streams</li> </ul> <p><b>INJECTION POINTS</b></p> <ul style="list-style-type: none"> <li>★ Uranine</li> <li>★ Sulfurhodamine G</li> <li>★ Tunnel sampling</li> </ul>
---	--	---	--



**Fig. 1** Hydrogeological map of the study area in the regions of Tuscany and Emilia-Romagna (*shaded grey in the index map*), with location of the Firenzuola tunnel and the four access windows, the impacted streams, wells and springs (with the names and IDs used in the text and following figures) and the injection and sampling sites of the two multi-tracer tests (geology simplified from CARG project survey; Carta Geologica d'Italia, National Geological Map of Italy, 1:50,000 scale, sheet 253 "Marradi", not yet published; courtesy of Geological, Seismic and Soil Service of Emilia-Romagna Region). *T1* and *T2* are thrust faults of particular relevance, *F1–F6* are normal faults; *dashed lines* indicate faults derived from geologic surveys inside the tunnel, *continuous lines* indicate faults that were previously known from geological mapping

(Bendkik et al. 1994; Boccaletti et al. 1997; Cerrina Feroni et al. 2002). Thrusts prevail north of the divide (T2 in Fig. 1); normal faults prevail to the south (F1–F6 in Fig. 1), due to the opening of the Mugello graben.

Turbidite formations, although widespread throughout the world, have not received much attention in the hydrogeological literature and are often not considered as relevant aquifers due to the high percentage of fine-grained components. However, in some regions, fractured turbidites represent important aquifers.

The mean precipitation in the region is 1569 mm/year (average value from 1960 to 2004); the years 1995 to 1998 were slightly drier, with an average of 1439 mm/year. The hydrologic year, which starts in October, presents a rainfall maximum during November to April and a drier season from May to October (Gargini et al. 2008).

A conceptual model of groundwater circulation in turbidites was recently proposed on the basis of a large quantity of hydrogeological monitoring data related to tunnel excavations (Gargini et al. 2008). According to this model, three main types of groundwater flow system (GFS) can be identified in turbidite aquifers:

**GFS 1:** Shallow groundwater circulation in the uppermost 100–200 m, where stress release has caused intense fracturing; regolith, landslide deposits and debris also belong to this zone. A shallow GFS largely follows the topography and discharges into many small springs (often < 1 L/s; ‘slope’ type spring, S) or streams.

**GFS 2:** Along major extensional structures (steep and relatively deep-reaching fracture zones), linear flow

systems develop, sometimes across several surface watersheds. These flow systems discharge to a few relatively large springs (mean discharge ranging from 1 L/s to > 10 L/s; ‘transwatershed’ type spring, T) or directly to streams (Fig. 2). Prior to tunnel excavation, all streams in the region (where turbidites outcrop) were gaining streams and were fed by GFS 1 and GFS 2, i.e. groundwater flow was oriented towards the streams, which is the typical setting for a mountainous landscape consisting of low to moderately permeable rocks under humid climatic conditions. Field observations and flow measurements support this evaluation (Gargini et al. 2006, 2008).

**GFS 3:** Deep regional circulation systems develop between the central parts of the mountain chain, where high recharge occurs, and the lower-lying areas at their margins. These flow systems often discharge into alluvial sediments or contribute to the baseflow of larger rivers in the deeply incised valleys. Discrete discharge points are rare and occur as sulphur-smelling springs.

### Impacts of the tunnel on groundwater and surface waters

During excavation, 14 major water intrusions into the main tunnel and the access windows occurred between 1999 and 2003. Peak inflows were within a range of 30 to more than 500 L/s. The total drainage during drilling advancement reached instantaneous flow rates of more than 1,000 L/s. Two years after completion of the Firenzuola

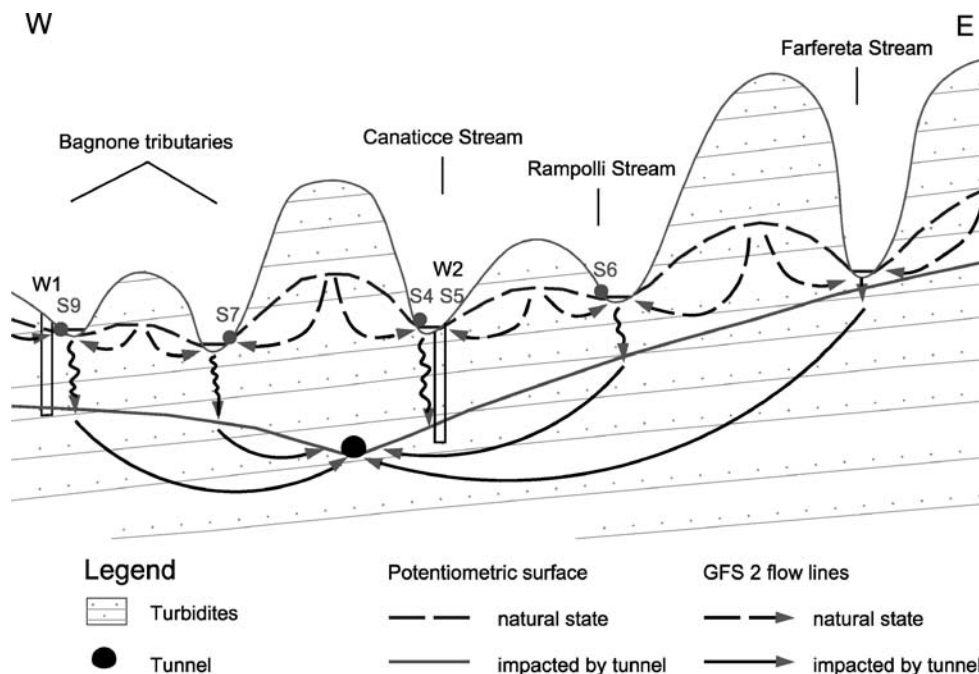


**Fig. 2** Conceptual model illustrating the impact of the tunnel on the groundwater and surface waters, as it was observed in the southern sector of the Firenzuola tunnel (modified after Gargini et al. 2008). The section is representative of the impacts that occurred along thrust fault T1 (west) and normal fault F1 (east). The filled circles represent impacted springs; the lag time and magnitude of the observed impact on the five shown streams depends on the distance to the tunnel. The section trace is shown in Fig. 1

tunnel, the average drainage outflow is 355 L/s with an evident relationship to the annual recharge regime: 210 L/s at the end of the recession period in autumn, but more than 400 L/s during winter (Gargini et al. 2008).

The main impacts on springs and streams occur in the zones consisting of turbidites with a high A/P ratio: the Nespoli member in the northern part and the Premilcuore member in the south. As a consequence, 12 springs (S1–S12 in Fig. 1) and five previously perennial streams (Rovigo and Veccione in the north; Bagnone, Bosso and Farfereta in the south) were completely or seasonally dried, with severe socio-economic and ecological effects such as the total disappearance of fish, amphibians and aquatic invertebrates in the dry stream sections. Although this type of impact has not been systematically monitored, it is obvious.

The mechanisms of the impact were different in the north and in the south, and were established by studying the space-time array of the inrush-impact relationships as derived by monitoring data collected by the Hydrological Monitoring Programme (HMP) performed by the constructors during drilling advancement.

In the southern part (Premilcuore member), the main inrushes occurred between p. 52+850 km and p. 54+450 km (Fig. 1), during the northward advancement of the Marzano window and the Firenzuola tunnel in 1999–2003, and are related to extensional fracture zones and faults parallel to the Mugello graben. All main springs aligned along these structures (T1, F1) were completely dried up and the disappearance of summer flow in the five impacted streams shown in Fig. 1 is mainly related to water losses in the intersection zones between the streams and the extensional faults F1 to F4. Starting from the rough data of the HMP (completed through surveys done by the authors in 2000–2002 and 2005–2007), the progressive development of the impact has been inferred (Fig. 3). Five main “impact events” can be identified from water inrushes during drilling advancement (Fig. 3b), increasing drawdown observed in wells (Fig. 3c), and decreasing spring and stream flows (Fig. 3c-e). Most of the impact events are related to tectonic extensional structures crossed by the tunnel, only two of which (F1 and F5) had been identified from the surface during geologic surveys before drilling:

1. In June 1999, a water inrush of 30 L/s in the access window (MW) at p. 54+450 km along the thrust T1 induced a sudden but small drawdown in a well (W1); after one year (July 2000) spring S9, located on the same structure, also became impacted.
2. In March 2000, the tunnel crossed the extensional fault F1, triggering a water inrush of 20 L/s at p. 54+130 km; the impact on the two spring S4 and S5 aligned along F1 was almost immediate (they dried up after 1 and 3 months, respectively).
3. From January to May 2001, the tunnel crossed F2 from p. 54+000 km to p. 53+800 km and several nearby water inrushes in the tunnel increased the total tunnel outflow by one order of magnitude and caused the lowering of the water levels in wells W1 and W2 and

the complete drying up of spring S6; these events impacted, for the first time, Rampolli Stream where section F became dry during the summer season.

4. Between March and December 2002, the tunnel crossed three extensional faults (F3, F4, F5), creating significant water inrushes which increased the total drainage by a factor of five; the quite immediate effect was evident at well W1 with the water level dropping 30 m more; no main springs are located along these structures and the impact involved mainly the baseflow of streams, reaching Farfereta Stream in July 2003.
5. Finally, the interception of F6 caused some water inrushes but no impacts were observed, because the upgradient streams and springs are located over a low permeability member of MAF, which separates the tunnel from the surface waters.

The hydrographs in Fig. 3 clearly display sudden declines of spring discharge, with relatively short time lags between the water inrush and the impact; varying from nearly instantaneous to some months, according to the distance of the spring from the tunnel along the fault. A hydraulic diffusivity estimate was made based on these time lags, resulting in a mean value of about 1,000 m/month (Gargini et al. 2008). Fast and intense impacts were also recorded on streams. However, the stream hydrographs consist of baseflow and direct flow, while the tunnel mainly reduces the baseflow, so the effects are evident mainly during recession periods.

In the northern part (Nespoli member), the main inrushes occurred between p. 45+900 km and p. 48+200 km (Fig. 1). Due to the absence of long and continuous extensional fracture zones, these inrushes can be explained as drainage from a decompressed and generally fractured rock mass extending down to 200 m depth. For the same reason, the drainage effect of the tunnel does not propagate for such long distances as in the southern part. Several slope springs and streams (e.g. Rovigo and Veccione) were impacted by the tunnel shortly after the water inrushes occurred. In a general way, the impact in the southern part corresponds to GFS type 2, while the impact in the north corresponds to GFS 1, as described above.

Figure 2 presents a conceptual model of the impact of the tunnel on groundwater and surface waters that matches observations in the southern part of the study area. The section runs along the faults, where higher permeability promotes drainage to the tunnel. The tunnel has completely altered the natural flow system. Before the tunnel was built, the water table was above the level of the streams, and the aquifer drained towards springs and streams. Now, the tunnel drains the entire system; the water table dropped below the valleys, drainage divides have lost their function and streams and springs run dry. However, a direct experimental proof for this conceptual model was missing. Therefore, a comprehensive experimental program was established in order to demonstrate and quantify the stream-aquifer-tunnel connections.

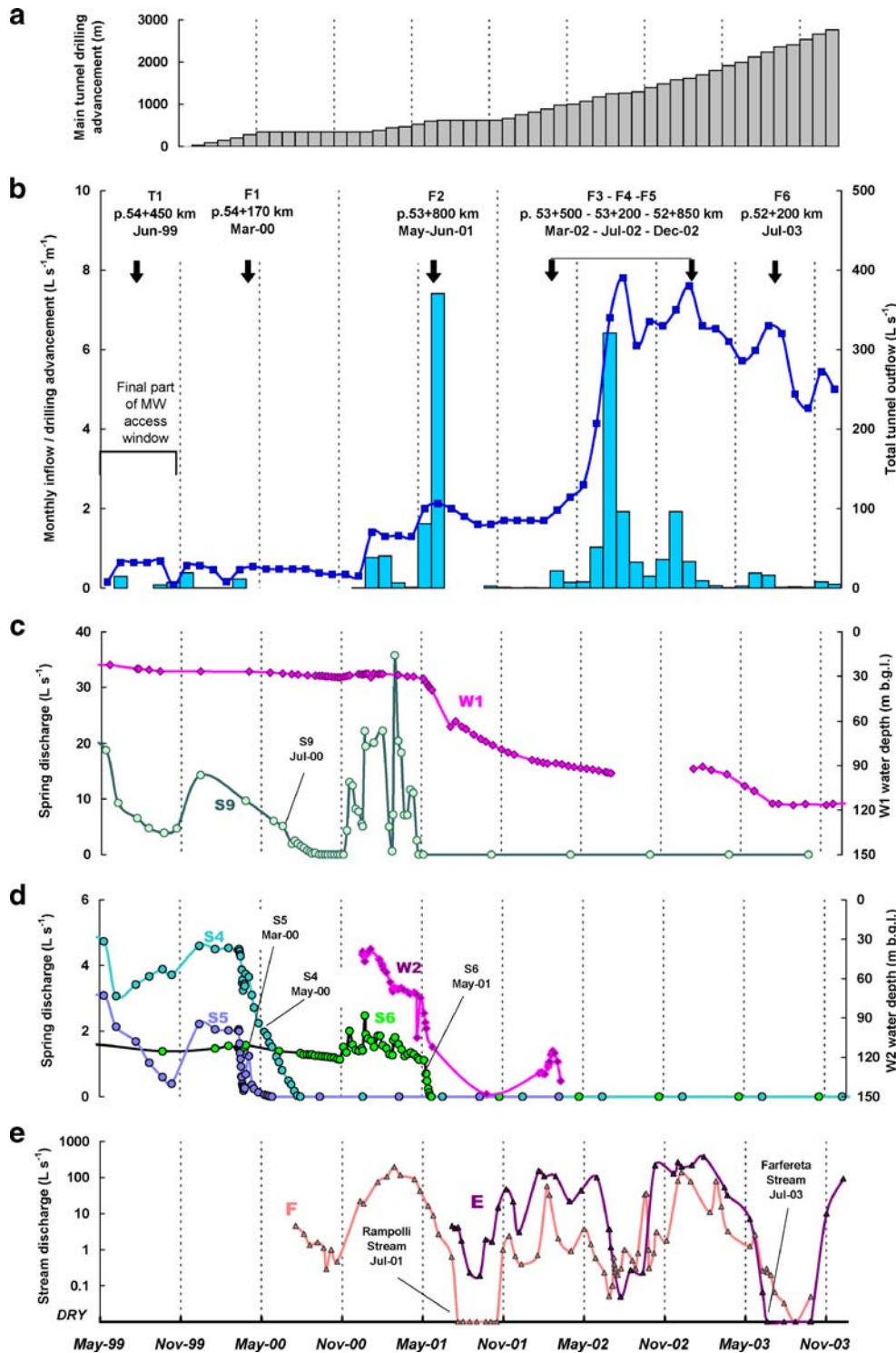


**Fig. 3** Detailed chronology of impacts on groundwater and surface waters in the southern sector of Firenzuola tunnel. **a** Drilling advancement of the main tunnel vs. time. **b** Monthly tunnel inflow normalised by meters of monthly drilling advancement, and total tunnel outflow vs. time, from p. 54+500 km to p. 51+627 km. **c** Chronology of impacts on spring *S9* and on well *W1* (western side of the tunnel). **d** Chronology of impacts on springs *S4*, *S5*, *S6* and on well *W2* (eastern side of the tunnel). All the springs have been completely dry since 2001. **e** Stream discharge vs. time at stream sections *F* (*Rampolli Stream*) and *E* (*Farfereta Stream*), eastern side of the tunnel. Since 2003, the two stream sections have been completely dry every summer

## Materials and methods

### General approach

Starting from the conceptual model presented in Fig. 2, the general approach was as follows:

1. Identification of the infiltration zones in the streambeds using existing hydrological data, observations made by local people and new detailed stream flow surveys (2001–2006)
2. Characterisation of water inlets in the tunnel, including the evaluation of existing data on water inrushes during the drilling and detailed surveys of water inlets that are still active
3. Demonstration and characterisation of the assumed stream-tunnel connections by means of multi-tracer tests with a total of four injection sites between different reaches of the stream network and the water inlets in the tunnel

### Stream flow surveys

The data collected within the HMP made it possible to identify the impacted stream sections only in a general way. However, in order to localise the most important infiltration zones in the streambeds and to characterise their evolution over the year, repeated and detailed stream surveys were done within the framework of this study, using the salt-dilution method of flow measurement (Käss 1998). For each measurement, an appropriate quantity of salt (~1 kg NaCl for an estimated 100 L/s) was dissolved in a bucket of water and injected into the stream. The specific electrical conductivity (SEC, in  $\mu\text{S}/\text{cm}$  at 25°C) was recorded with a CTD diver 20 to 120 m downstream, where the salt plume had completely mixed with the stream. The natural background was subtracted from the measured SEC, and the salt concentration ( $c$ ) was determined using an empirical correlation between  $c$  and SEC that was established for each stream. Finally, the stream discharge was obtained by dividing the injected salt mass by the surface area below the breakthrough curve.

### Flow measurements inside the tunnel

The monitoring sites in the Firenzuola tunnel are determined by the installed drainage system. To avoid uncontrolled water inflows into the tunnel, there is a waterproof PVC foil between the concrete lining and the fractured rock. Every 25 m, on both sides of the tunnel, a group of 25 m long full-screened tubes drain water towards an inspection well. Two pipes at the base of each tunnel sidewall collect the water and convey it towards the tunnel portals.

The discharge at the sampled drainage tubes was measured using a bucket and a stopwatch. The total discharge at the tunnel portals is measured automatically and continuously by the constructor. On the northern side,

a laser system measures water level at a calibrated weir; on the southern side, a magnetic flowmeter is installed at the collecting pipe.

### Tracer tests

Two multi-tracer tests, with two tracers in each case, were done in two streams impacted by the tunnel, Rampolli Stream in the southern part of the area and Veccione Stream further to the north. Because of the expected long travel times, high dilutions and high dispersivities of the tracers, relatively high injection quantities were required, resulting in high concentrations in the stream water. Therefore, ecotoxicological safety was a major selection criterion for the tracers. The fluorescent dyes uranine (CAS 518-47-8) and sulforhodamine G (CAS 5873-16-5) were selected as tracers, because of their favourable properties (Käss 1998) and proven safety (Behrens et al. 2001).

All tracers were dissolved on-site in different barrels of stream water (~100 L) and then poured into the flowing stream. As fluorescent dyes are sensitive to sunlight, the injections were done in the evening. The tracers were instantaneous released in the streams (~1 h), but the effective duration of the injection into the aquifer was much longer, as there was intermediate storage of tracer in pools of the slow-flowing streams.

On 6 May 2006, 1 kg of sulforhodamine G was injected into a tributary of the lower part of Rampolli Stream, some tens of metres upstream from the confluence point with the dry Rampolli streambed; 5 kg of uranine were injected further upstream (Figs. 1 and 5); the two parts of the stream were separated by a dry section, ensuring separation of the two tracer injections. On 13 December 2006, 8 kg of sulforhodamine G was injected in the middle part of Veccione Stream and 10 kg of uranine were injected further upstream (Figs. 1 and 6). There was continuous flow between the two injection points, so that uranine was dispersed in the entire stream, while sulforhodamine G only labelled the lower section of the stream.

Monitoring inside the tunnel included both discrete water sampling (manually and with auto-samplers) and accumulative sampling by means of activated charcoal bags. Blank samples were taken prior to injections and all were negative. The sampling surveys involved both single points (i.e. inspection wells or water inlets at fissures in the concrete) and integral points (i.e. the central trench or the big pipes conveying waters outside, including all the water collected further upgradient). During the experiment, the monitoring program was continuously modified and optimised, as a function of the intermediate results.

The southern part of the tunnel (Firenzuola S) was sampled 32 times between 6 May 2006 and 30 March 2007. In total, there are 50 sampling points in this 2,865 m long part of the tunnel (Figs. 1 and 5). The total number of analyses was 1550 for water samples and 930 for charcoal bags. The northern sector (Firenzuola N) is 7,236 m long (Figs. 1 and 6) and was sampled 23 times between 30 November 2006 and 13 April 2007, when work inside the tunnel made further sampling impossible. For this exper-

iment, 96 sites were sampled; 2,304 water samples and 185 charcoal bags were analysed (only from sites where water samples were negative). By means of an on-line fluorometer (Schneegg and Flynn 2002), the two tracers were continuously monitored in the total water outflow at the northern entrance of the tunnel.

The samples were analysed with a spectrofluorometer (PerkinElmer LS 45). As the tunnel drip waters have a pH >8, it was not necessary to add a basic buffer to the water samples. Charcoal samples were dried, dipped in an eluent for 12–14 h (10 g KOH per 100 ml of 96% ethanol) and then analysed with the spectrofluorometer (Käss 1998).

### Evaluation and analysis of the tracer breakthrough curves

Tracer results are presented as concentration-time data, i.e. breakthrough curves (BTCs). Basic parameters were directly obtained from the BTCs: first detection time ( $t_1$ ), peak time ( $t_p$ ), peak concentration ( $c_p$ ), and the corresponding maximum velocity ( $v_{max}$ ) and peak velocity ( $v_p$ ). The minimum three-dimensional distances between the stream and the tunnel were taken as relevant flowpath length ( $L$ ). For the southern sector, the minimum three-dimensional distances were considered along the main faults; for the northern sector, where such prominent faults are absent, the distances have been considered perpendicular to the tunnel. Tracer recoveries ( $R$ ) were calculated as a function of the variable discharge ( $Q$ ).

Mathematical models make it possible to obtain more advanced transport parameters by fitting a solution of a differential transport equation to the observed data. Different analytical solutions are available for a wide range of hydrogeological settings with well-defined initial and boundary conditions (Bear 1979; Toride et al. 1993).

In the present case, the tracer pathways include a passage in surface streams followed by transport through a network of unsaturated and saturated fractures towards the tunnel. There is no mathematical solution for such a complex system. In order to obtain at least some global indications on the transport processes and to be able to compare the

different tracer results, the simplest analytical solution was fitted to the observed data: the conventional one-dimensional advection-dispersion model (ADM; Kreft and Zuber 1978). The ADM requires two fit parameters: advection is expressed as mean transit time ( $t_0$ ) or mean flow velocity ( $v$ ); dispersion can be expressed as dispersion coefficient ( $D$ ) or dispersivity ( $\alpha=D/v$ ). CXTFIT (Toride et al. 1999) was used to fit the analytical model to the data.

## Results and discussion

### Evolution of the impact on streams

The flow measurement data derived from the HMP allowed the comparison of the mean baseflow of the different streams before the tunnel was drilled (1995–1998) with the baseflow after the tunnel drilling (2005–2006) thus providing the consequent estimate of the baseflow loss. For the calculation of the baseflow values, only stream discharge measurements made after at least 5 days from the last rain have been considered.

The baseflow losses range from 40 to 84% (Table 1). The highest value corresponds to Bosso Stream; dramatic losses (65%) have also been observed in the Veccione Stream (section B in Fig. 1), a tributary of Rovigo Stream. The slight decrease of total annual rainfall (8% less rainfall in 2005–2006 compared to 1995–1998) is not sufficient to explain this substantial baseflow loss, which can mainly be attributed to drainage into the tunnel. The total baseflow loss is 254 L/s, less than the total outflow of the tunnel (355 L/s in 2005–2006), suggesting that the system is still in a transient state and further impacts have to be expected.

On the northern side, Veccione Stream is most severely impacted by the tunnel, as well as the lower reaches of Rovigo Stream, which are directly located above the tunnel, and where rock coverage is thin, so that the stream-tunnel connections are obvious.

The tunnel crosses the Veccione watershed over a length of 5.5 km. At two places, the tunnel passes directly under the stream: at p. 49+000 km (main tunnel) and near p. 50+000 km (access window; Fig. 1). The impacts are not

**Table 1** Baseflow loss estimation for the streams impacted by Firenzuola tunnel compared to rainfall data (data of stream flow during dry periods from HMP; precipitation measured at Barco rainfall gauge; location of stream sections and rain gauge in Fig. 1). The slight decrease of annual rainfall of 8% cannot explain the baseflow loss of 40–84%

Stream section		Average baseflow (L/s)		Baseflow loss	
		Natural conditions (1995–1998)	Impacted by tunnel (2005–2006)	(L/s)	(%)
Northern sector	Rovigo Stream (A)	356	190	166	47
Southern sector	Bagnone Stream (C)	11	6	5	45
	Bosso Stream (D)	92	15	77	84
	Farfereta Stream (E)	15	9	6	40
Total		474	220	254	54
		Rainfall (mm/year)		Rainfall decrease	
		1,439	1,325	114	8

restricted to these zones but the stream flow surveys revealed significant seepage losses along most of the stream. In June 2006, the discharge decreased from 60 to 30 L/s in the middle section of the stream (near p. 49+000 km) and from 46 to 25 L/s in the lower section (near km 47) within 11 days, demonstrating that the gaining stream had trans-

formed into a losing stream (Fig. 4a). On 18 July 2006, the stream started to dry up in the lower section, and the dry part slowly propagated upstream. In September, the entire lower and middle section of the stream was dry until the beginning of December due to a particularly dry autumn.

In the southern part of the area, several watersheds are impacted by the tunnel (Fig. 1). The most severe impacts can be observed in two tributaries of Bosso Stream. Already during springtime, the western tributary (Canaticce) runs completely dry in its entire lower part, thereby exterminating all active aquatic life in this previously permanent stream. The eastern tributary (Rampolli) also runs dry during summer in its lower part, although the springs in its upper part maintain their flow rates, indicating seepage losses further downstream. Figure 4b illustrates the temporal evolution of the flow rates along Rampolli Stream: the two infiltration zones, where the drying up starts in early June, seem to be related with two tectonic structures (T1 and F1). In the following weeks, the dry part of the stream migrates progressively upstream, due to additional infiltration zones. During summer, the stream remains dry until intense rainfall and recharge restarts in autumn or winter.

Based on these examples and other stream surveys, several hypotheses can be formulated:

- As the tunnel continues to drain the aquifer, the impact on the streams gets worse every year, indicating that steady state has not yet been reached.
- Where seepage losses are localised at distinct tectonic structures (faults and fracture zones), as in the case of Rampolli Stream, dryness starts at these points, suggesting that these structures also constitute the principal stream-tunnel connections.
- Where fracturing and seepage losses are more dispersed, as in the case of Veccione Stream, dryness starts in the lower section of the stream and then propagates upstream.

Although the stream flow survey further confirms the conceptual model of regional groundwater drainage by the tunnel, only tracer tests can deliver clear evidence.

### Stream-tunnel connections demonstrated by tracer tests

The uranine that was injected in the upper section of Rampolli Stream was detected at several sampling sites in the southern part of the tunnel, 18 to 74 days (d) after the injection (Table 2, Fig. 5). The stream is located east of the tunnel, but the tracer arrived on both sides, which can be explained by over- or underflow; this was possible due to the presence of a “controlled drainage system”, implemented by the tunnelling company (since 2005) in order to elevate the groundwater level above the tunnel in order to decrease the hydraulic gradient and the tunnel discharge rate. Four main stream-tunnel connections can be identified:

1. Where the tunnel crosses the extensional fault F2: uranine detection at sampling site 3DX (first arrival after 35 d) proves direct connection between the stream

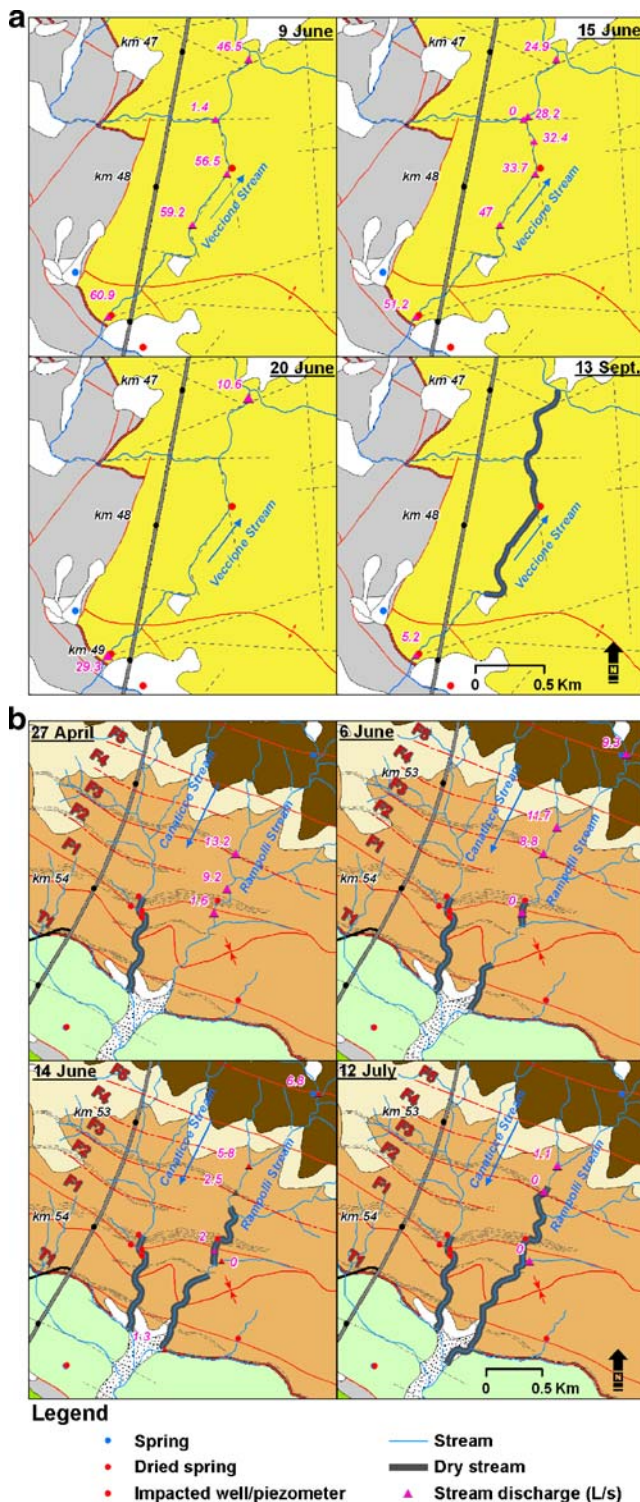


Fig. 4 Temporal evolution of the drying up process of a Veccione Stream and b Rampolli Stream in 2006. The legend for geological and other features is shown in Fig. 1

**Table 2** Summary of uranine tracer test results: minimum three-dimensional distance between stream and sampling point inside the tunnel ( $L$ ), discharge of water inlet ( $Q$ ), time of first detection ( $t_1$ ), peak time ( $t_p$ ), peak concentration ( $c_p$ ), and the corresponding maximum velocity ( $v_{max}$ ) and peak velocity ( $v_p$ ), tracer recoveries ( $R$ ), as well as the velocity ( $v$ ) and dispersivities ( $\alpha$ ) and regression coefficient ( $R^2$ ) obtained by modelling (ADM);  $ND$  not determined,  $NA$  not applicable. The table shows the results obtained at 20 representative tracer arrival points: 12 of 35 from the northern sector of the tunnel and 8 of 13 from the southern sector

	ID water inlet	Basic data								ADM		
		$L$ (m)	$Q$ (L/min)	$t_1$ (d after injection)	$t_p$ (d after injection)	$c_p$ ( $\mu\text{g/L}$ )	$v_{max}$ (m/d)	$v_p$ (m/d)	$R$ (g)	$v$ (m/d)	$\alpha$ (m)	$R^2$
Northern sector	9DX	117	1	1	2	4.33	116.8	58.4	0.02	42.3	14.7	0.962
	20DX	135	6	1	2	6.72	135.4	67.7	0.39	28.7	27.4	0.929
	RW	94	420	1	1	5.66	94.0	94.0	9.17	NA	NA	NA
	83SX	373	156	17	45	0.13	21.9	8.3	1.71	5.8	68.7	0.983
	85SXm	373	30	17	45	0.15	22.0	8.3	0.39	5.2	89.2	0.901
	85SXv	373	135	17	50	0.13	22.0	7.5	1.53	5.2	87.8	0.960
	88SX	403	40	17	45	0.12	23.7	9.0	0.37	5.8	65.1	0.970
	89SX	403	34	17	45	0.12	23.7	9.0	0.31	5.6	68.8	0.960
	111SX	468	175	30	91	0.05	15.6	5.1	0.64	3.0	74.0	0.987
	141SX	203	3	8	26	0.90	25.4	7.8	0.21	3.1	82.6	0.965
	141DX	203	2	8	30	0.55	25.4	6.8	0.08	2.8	60.8	0.901
	148SX	206	4	8	30	0.36	25.8	6.9	0.15	1.0	239.0	0.968
	OSTDX	91	600	4	17	5.12	22.8	5.4	216	1.5	40.2	0.970
	Southern sector	3DX	1,114	ND	35	ND	ND	31.8	ND	ND	NA	NA
4DX		1,140	ND	18	56	0.37	63.3	20.4	ND	5.5	574.9	0.950
30DX		1,110	ND	ND	69	0.28	ND	16.1	ND	14.4	25.2	0.870
25DX		1,107	ND	ND	53	0.07	ND	20.9	ND	18.7	44.9	0.799
6DX <sup>a</sup>		1,113	ND	35	ND	ND	31.8	ND	ND	NA	NA	NA
7DXv		1,122	ND	47	ND	ND	23.9	ND	ND	5.7	123.8	0.730
7DXm		1,122	ND	47	ND	ND	23.9	ND	ND	10.1	21.7	0.817
10DX <sup>a</sup>		1,348	ND	69	ND	ND	19.5	ND	ND	NA	NA	NA
12DX <sup>a</sup>		1,390	ND	74	ND	ND	18.8	ND	ND	NA	NA	NA

<sup>a</sup> Only charcoal bags were positive

segment that runs dry first during springtime (Fig. 4b) and the 500 L/s water inlet (maximum flow during drilling) in the tunnel (Fig. 5b).

- The narrow zone between F2 and F3: uranine detection at 4DX 18 days after injection corresponds to the highest observed maximum velocity, 63 m/d. The tracer also arrived at the nearby sampling points 25DX, 25 SX, 30DX and 30SX. Probably, the tracer travels first along fault F2 but then follows the dip of the strata towards the sampling points; another reason could be a densely fractured zone between the two faults.
- Several arrival points around the fault F4 showed positive results about 40 d after injection.
- Two arrival points are related to F5: uranine arrived after about 70 d at 10DX and 12DX, but was only detectable in charcoal bags. This connection follows a fault and fracture zone that is visible both at the surface stream and in the tunnel; it represents the longest traced distance (1.4 km) but also the lowest maximum velocities (18.8–19.5 m/d).

Sulforhodamine G injected in the lower reach of Rampolli Stream, down gradient to the dry reach, was not detected at any of the sampling sites. This can be explained by the relatively low injection quantity (1 kg), the properties of the tracer, which is more prone to adsorption than uranine (Käss 1998), and/or a less developed stream-tunnel connection.

At the Veccione test site, both tracers injected into the stream were detected at numerous sampling sites in the

northern sector of the tunnel (Table 2, Fig. 6). In general, uranine delivered better results, i.e. a greater number of positive detections and breakthrough curves with clearer peaks and shorter tails, demonstrating a more conservative behaviour than sulforhodamine G (Fig. 7). In general, the tracers arrived only on the side of the tunnel that is oriented towards the stream, indicating that the tunnel separates the aquifer. Only near p. 49+000 km, where the tunnel passes below the stream, was uranine detected on both sides of the tunnel. Despite the large number of positive sampling sites, four main connection zones can be identified:

- Lower part of Rovigo Stream: uranine arrived in the shortest times (1–2 d), with highest velocities and highest concentrations (up to 10 ppb). Eleven positive detections in this sector are located on the western side of the main tunnel.
- Confluence of Veccione and Rovigo streams: the highest water inflows into the tunnel occur in a 300-m-long sector near the confluence point. Uranine arrived after 17 d, with a maximum velocity of 20 m/d and concentrations < 0.14 ppb. Eight positive detections are located on the eastern side of the tunnel, which coincides with the geometry of the stream.
- Veccione valley from p. 47+500 km to p. 49+000 km: thirteen arrival points are dispersed along this reach (eight on the eastern side and five on the western one), not clearly related to any particular tectonic structures; the first detections occurred after 8 days, with similar concentrations to those in zone 2.

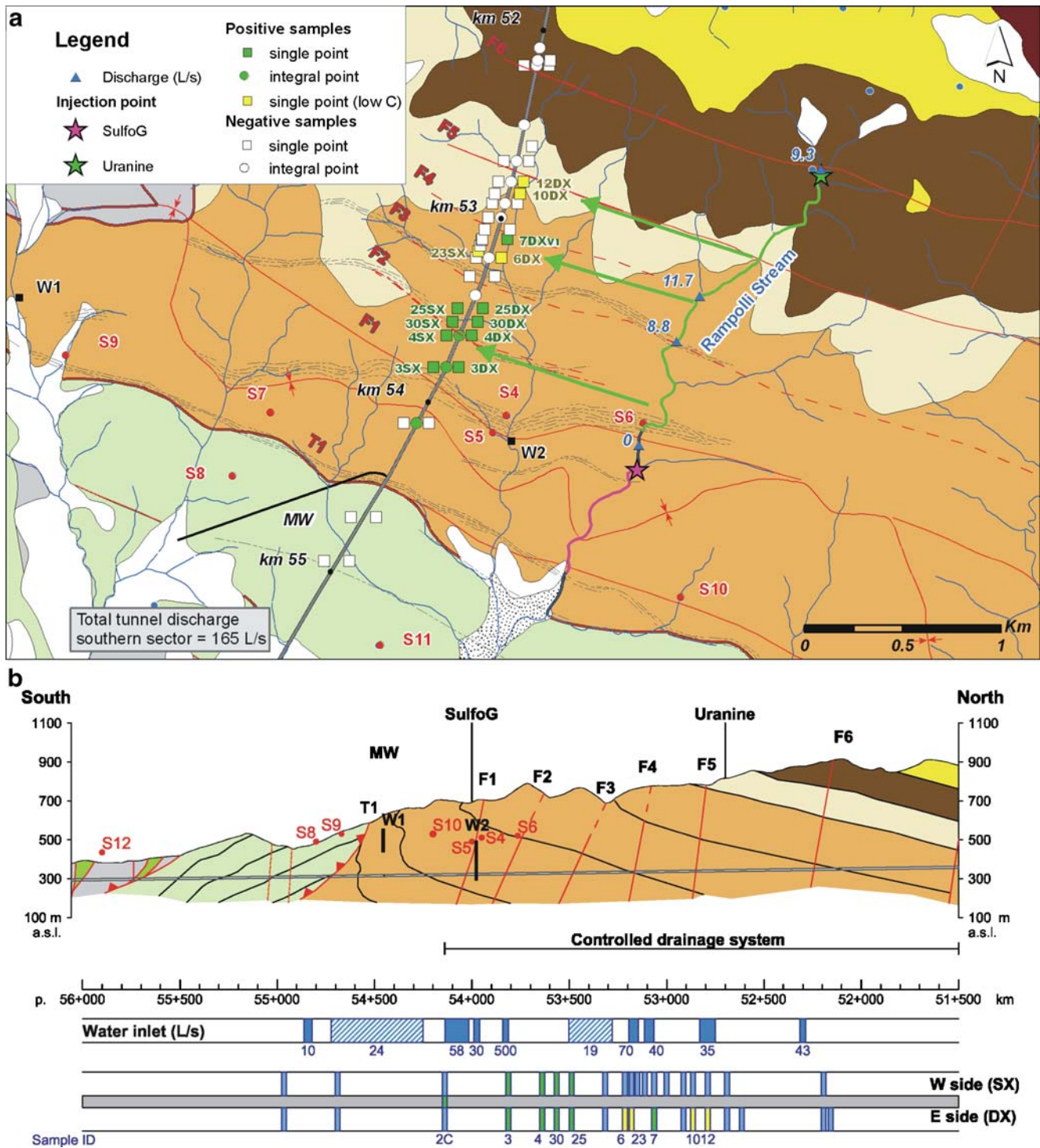


**Fig. 5** Results of the tracer test between Rampolli Stream and the southern sector of the tunnel: **a** map with location of injection points in streams, the sampled water inlets in the tunnel (positive or negative) and the main connections identified; **b** geological profile along the tunnel, with topographic elevations of impacted springs (S) and wells (W) projected onto the relevant sections of tunnel. The chronology of impacts is shown in Fig. 3. The first bar below the profile in **b** represents the maximum water inflows measured during drilling advancement; the lower double bar represents the sampling points (SX and DX) on both sides inside the tunnel during the tracer test and the results obtained with uranine (green: positive detections; yellow: positive but low concentrations; blue: negative results). Sulforhodamine G (SulfoG) was not detected at any sampling site inside the tunnel. The geological legend is shown in Fig. 1

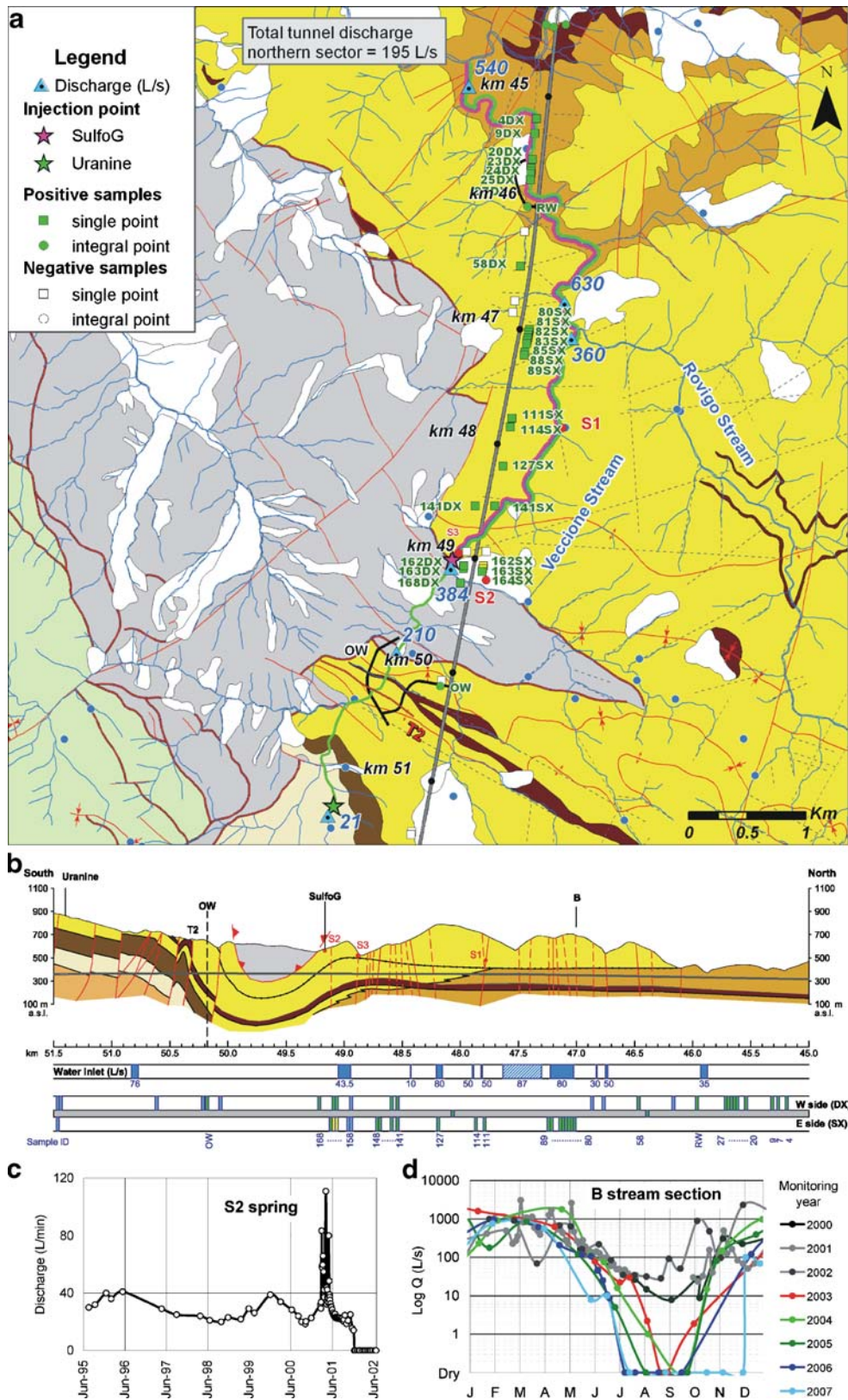


**Fig. 6** Results of the tracer test between Veccione Stream and the northern sector of the tunnel: **a** map with the injection points, sampling sites and proven connections; **b** geological profile along the tunnel with topographic elevations of impacted springs (S) projected onto the relevant sections of tunnel; for explanation of the bars below the profile see caption of Fig. 5; **c** hydrograph of spring S2 (completely dry since summer 2002) and **d** hydrographs of B section (Veccione Stream) from 2000 to 2007 are shown to illustrate the impact

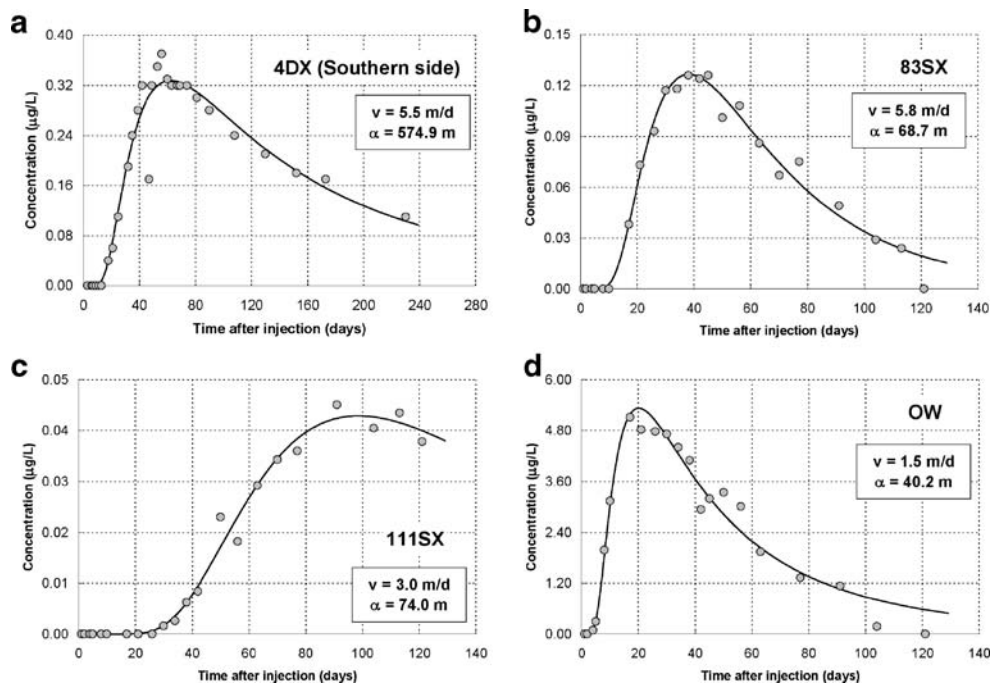


**Fig. 7** Selected uranine breakthrough curves **a** from the southern section of Firenzuola tunnel, resulting from the injection into Rampolli Stream and **b–d** from the northern section, resulting from the injection into Veccione Stream; *open circles*: measured concentrations; *line*: simulated breakthrough curve (ADM). The injection and samplings sites are shown in Figs. 5 and 6; the simulation data and results are presented in Table 2

- The integral water sample (i.e. sample taken at a collector that includes water from all outlets further upgradient) from the access window OW was also positive for uranine, indicating a stream tunnel connection along the thrust fault T2.

The tracer recoveries were generally low: 2.3% of the uranine injected into Veccione Stream was recovered in the northern sector of the tunnel; the recoveries of the other experiments were even lower or undetermined, as it was not possible to measure flow rates at all sampling sites (Table 2); furthermore, some connections were only proven by charcoal samples. The low recoveries can be explained by the experimental and hydrogeological conditions such as injection into surface streams, double-porosity effects and retardation in the unsaturated zone and aquifer, and difficult sampling and monitoring conditions in the tunnel.

### Evaluation of the breakthrough curves and the flow system

Table 2 presents a summary of the most relevant tracer results from the northern and southern part of the area, as obtained from the observed BTCs and the modelling results (ADM). Figures 7 and 8 show selected BTCs. The highest flow velocities occurred in the far north, where the tunnel is closely below Rovigo Stream: 135.4 m/d on a distance of 135 m. Apart from these exceptionally high flow velocities, there are systematic difference between the north and the south.

In the south (Rampolli Stream), the linear flowpath lengths proven by the tracer test are more than 1 km (1,107–1,390 m); the maximum flow velocities range between 18.8 and 63.3 m/d; peak velocities are 16.1–20.9 m/d, and the mean velocities obtained from the ADM are 5.5–18.7 m/d. The most direct connection and the most complete BTC were established at F4DX (Fig. 7a), and the most reliable modelling results were obtained for this BTC, documented by a relatively high coefficient of determination ( $R^2=0.95$ ). The simulation revealed a very high longitudinal dispersion coefficient ( $D=3,162 \text{ m}^2/\text{d}$ ) and longitudinal dispersivity ( $\alpha=574.9 \text{ m}$ ). Although the investigated flow system is highly complex and cannot be sufficiently simulated by a simple ADM, the high dispersivity indicates a great variance of flowpaths and flow velocities in the stream and fractured turbidite rocks. Simulation of the other BTCs yields lower dispersivities, but the results are less reliable. In the north (Veccione Stream), the distances confirmed by the tracer test are much shorter (91–468 m) and the flow velocities are generally lower (with the exception mentioned above). The maximum flow velocities range between 8.8 and 23 m/d; the peak velocities are 2.1–8.7 m/d and the mean velocities are 0.6–5.6 m/d.

The tectonic structures explain the significant differences observed between the northern and the southern part of the area. In the south, long extensional faults and fracture zones connect the streams and the tunnel. Therefore, the impact propagates over large distances and crosses the borders of several watersheds; the tracer arrived at relatively few sampling sites, but travelled over

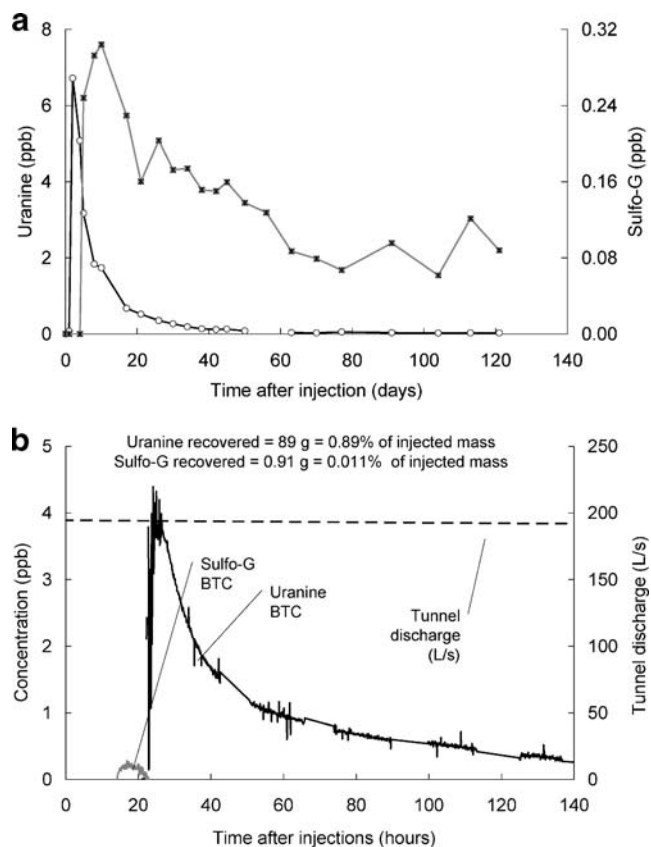


**Fig. 8** Comparison of uranine and sulforhodamine G. **a** BTCs measured at inspection well 20DX inside the tunnel: the uranine BTC shows 20 times higher maximum concentrations and a shorter tail than the sulforhodamine G curve, although uranine was injected further upstream in Veccione Stream, suggesting that uranine behaves more conservatively in fractured turbidites (injection and sampling site are shown in Fig. 6). **b** Uranine and sulforhodamine G BTCs measured by means of a continuous fluorometer at the total drainage of the northern sector of the tunnel. The uranine recovery is about 100 times higher than the sulforhodamine G recovery, further confirming the more conservative behaviour of uranine

large distances (> 1 km) and at high maximum flow velocities (up to 63 m/d). In the north, the seepage from the streams to the tunnel is distributed over many fractures, as demonstrated by the large number of tracer arrival points in the tunnel. The proven connections in this zone are shorter (< 500 m) and maximum flow velocities are slower (generally < 26 m/d), with the exception of some short and rapid connections in a zone where the tunnel is directly below the stream in a highly fractured zone. Therefore, the tracer tests have also confirmed that there is a permeability gradient from north to south, because of an increasing A/P ratio of the turbidite rocks and an increasing intensity of extensional faulting towards the south.

## Conclusions and outlook

The tracer tests confirmed that the Firenzuola high-speed railway tunnel drains the groundwater and surface waters in the region and has entirely altered the natural flow

system. Before the tunnel was drilled, the fractured turbidite aquifer discharged towards small springs and mountain streams, and surface and groundwater divides largely coincided with topographic divides. Now, the tunnel has lowered the water table below the level of the streams, causing inversion of the natural groundwater-surface water interactions: gaining streams have transformed into perched and losing streams. The conceptual model concerning the impact of the tunnel proposed by Gargini et al. (2008) and shown in Fig. 2 was fully confirmed.

Significant differences were observed between the northern and the southern sector of the area: the higher velocities and longer distances travelled by the tracers in the southern sector confirm the higher permeability of the turbidites in this zone and also explain the larger tunnel interference radius.

The detailed stream flow surveys done before and after the tunnel drilling made it possible to quantify the total baseflow loss: 254 L/s. As the total tunnel outflow (355 L/s in 2005–2006) is higher than this value, further baseflow losses have to be expected, i.e. the system has not yet reached a steady state. The slightly lower annual precipitation during these years cannot explain the dramatic baseflow loss.

The drying up of streams and springs has severe socio-economic and ecological consequences that were, however, not studied within the framework of this project, which focused on the hydrogeological aspects. As the groundwater level has been lowered by about 100 m, the vegetation on the lower slopes, in the valleys and near the streams has probably lost contact with the groundwater, which may alter the plant communities. The most severe ecological impact is on the fauna in the streams, including fish, aquatic invertebrates and different type of larvae. Although this impact has unfortunately not been monitored, it is quite obvious and can also be deduced from studies focusing on the impact of droughts on stream fauna (e.g. Reznickova et al. 2007). The type and degree of ecological impact depends on the type and degree of hydrological depletion. In stream sections that ran completely dry, all aquatic fauna has obviously disappeared. In periodically dry sections and where discharge has substantially decreased, the species spectrum is expected to change in order to adapt to the new conditions, but species that rely on permanently flowing water and high flow rates have disappeared or will disappear as the drainage by the tunnel continues.

Obviously, the construction of the tunnel was based on incorrect assumptions. The turbidite formations were previously not considered as aquifers, partly because there are generally only few hydrogeological studies dealing with turbidite rocks and partly because the potential impact of the tunnel on the groundwater and surface waters in the region was not sufficiently and thoroughly studied before the tunnel was drilled.

Now, the damage has been done, and restoration is not possible as long as the tunnel continues to drain the aquifer. Flow measurements and monitoring indicate that a

steady state has not yet been reached, so the situation may get worse. Several mitigation strategies are discussed in order to preserve at least a minimum stream flow:

- From the surface: local streambed sealing or bypass conduits in zones of preferred infiltration, e.g. where important extensional fractures and faults cross the streams. However, the main problem is not the infiltration of stream water into the underground, but the regional groundwater drawdown that has eliminated stream baseflow.
- From the tunnels to the surface: pumping of the drainage water to the upper sections of the impacted streams. This is highly energy consuming, and the chemical water quality of the drainage water is not the same as the initial stream water composition.
- From inside the tunnels: control of drainage by closing drainage tubes and monitoring water pressure above the concrete ('controlled drainage'). Reducing the drainage by the tunnel is actually an important measure. However, the impermeable linings of the tunnel cannot withstand high water pressures.

Apart from these main conclusions, the study also revealed several other findings of general relevance concerning the employed methodology and the hydrogeology of turbidite formations. It was possible to show that tracer tests are a feasible technique to study the hydrogeological impacts of tunnels. Otz et al. (2003) also did tracer tests between the land surface and monitoring points in an exploratory gallery built to test the potential impact of the Swiss Alp-Transit tunnel. However, they only detected minor traces at a few sampling points and concluded that there is no significant surface-tunnel connection.

After a first qualitative experiment in 2002, conducted in order to test the methodology applicability (Gargini et al. 2008), the experiments reported here are the first large-scale quantitative tracer tests in turbidite rocks that allow sharpening of the methodology and characterization of the flow systems. As indicated in the introduction, several other tracer tests have been realized in other catchments impacted by the tunnels. Uranine always delivered the best results. The tracer tests with tinopal CBS-X, LiCl and KI entirely failed, probably because of the higher detection limits and/or less favourable transport properties. The tracer test with sulforhodamine G described in this study was successful, but the analysis of the breakthrough curves clearly showed significant adsorption compared to uranine. A tracer test with sulforhodamine G in another catchment failed. In karst aquifer systems, a wide range of tracers can be used (e.g. Goldscheider 2005), while turbidite rocks seem to require a more careful selection of tracers. Based on the experiences presented here, only uranine can be recommended for large-scale tracer tests in turbidite formations.

To date, very few studies focus on the hydrogeology of turbidite formations and flysch environments, often on the scale of entire sedimentary basins such as the Swiss

Molasse Basin (Keller 1992) and the Central North Slope foreland basin, Alaska (Nunn et al. 2005). The study reported here is among the few that investigates experimentally the hydrogeology of turbidite formations on a catchment scale and the tracer tests delivered quantitative information on the flow directions and flow velocities in fractured turbidite sandstones.

**Acknowledgements** The authors gratefully acknowledge Florence County Government for financing the study; the tunnelling company CAVET for hydrological monitoring (HMP) and drilling advancement data and for allowing sampling inside the tunnels; Geologic, Seismic and Soil Service of Emilia-Romagna Region for geological cartography. A special thanks to all the people who took part in the field activities and to Dr. T. Bechtel (Lancaster, Pennsylvania, USA) for checking the manuscript.

## References

- Amy LA, Talling PJ (2006) Anatomy of turbidites and linked debrites based on long distance (120 x 30km) bed correlation, Marnoso Arenacea Formation, Northern Apennines, Italy. *Sedimentology* 53:161–212
- Atkinson JH, Mair RJ (1983) Loads on leaking and watertight tunnel linings, sewers and buried pipes due to groundwater. *Geotechnique* 33(3):341–344
- Bear J (1979) *Hydraulics of groundwater*. McGraw-Hill, New York, 567 pp
- Behrens H, Beims U, Dieter H, Dietze G, Eikmann T, Grummt T, Hanisch H, Henseling H, Käss W, Kerndorff H, Leibundgut C, Müller-Wegener U, Ronnefahrt I, Scharenberg B, Schleyer R, Scholz W, Tilkes F (2001) Toxicological and ecotoxicological assessment of water tracers. *Hydrogeol J* 9(3):321–325
- Bendkik AM, Boccaletti M, Bonini M, Poccianti C, Sani F (1994) Structural evolution of the outer Apennine chain (Firenzuola-Città di Castello sector and Montefeltro area, Tuscan-Romagnan and Umbro-Marchean Apennine). *Mem Soc Geol It* 48:515–522
- Boccaletti M, Gianelli G, Sani F (1997) Tectonic regime, granite emplacement and crustal structure in the inner zone of the Northern Apennines (Tuscany, Italy): a new hypothesis. *Tectonophysics* 270:127–143
- Cerrina Feroni A, Martelli L, Martinelli P and Ottria G, con contributi di Catanzariti R (2002) Carta geologico-strutturale dell'Appennino emiliano-romagnolo in scala 1:250.000. (Geologic-structural map of the Apennines of Emilia-Romagna region, at scale 1:250,000). Regione Emilia-Romagna - CNR, Pisa. S.EL.CA., Florence
- Cesano D, Olofsson B, Bagtzoglou AC (2000) Parameters regulating groundwater inflows into hard rock tunnels: a statistical study of the Bolmen Tunnel in southern Sweden. *Tunn Undergr Space Technol* 15(2):153–165
- Cibin U, Di Giulio A, Martelli L, Catanzariti R, Poccianti C, Rosselli S, Sani F (2004) Factors controlling foredeep turbidite deposition: the case of Northern Apennines (Oligo-Miocene, Italy). In: Lomas SA, Joseph P (eds) *Confined turbidite systems*. *Geol Soc Lond Spec Publ* 222:115–134
- Day MJ (2004) Karstic problems in the construction of Milwaukee's Deep Tunnels. *Environ Geol* 45(6):859–863
- Feinstein DT, Dunning CP, Hunt RJ, Krohelski JT (2003) Stepwise use of GFLOW and MODFLOW to determine relative importance of shallow and deep receptors. *Ground Water* 41(2):190–199
- Gargini A, Piccinini L, Martelli L, Rosselli S, Bencini A, Messina A, Canuti P (2006) Hydrogeology of turbidites: a conceptual model derived by the geological survey of Tuscan-Emilian Apennines and the environmental monitoring for the high speed railway tunnel connection between Florence and Bologna. *Boll Soc Geol Ital* 125:293–327

- Gargini A, Vincenzi V, Piccinini L, Zuppi GM, Canuti P (2008) Groundwater flow systems in turbidites of the Northern Apennines (Italy): natural discharge and high speed railway tunnel drainage. *Hydrogeol J* (in press). doi:10.1007/s10040-008-0352-8
- Goldscheider N (2005) Fold structure and underground drainage pattern in the alpine karst system Hochifen-Gottesacker. *Eclogae Geol Helv* 98(1):1–17
- Goodman RF, Moye DG, Van Schaikwyk A, Javandel I (1965) Ground water inflows during tunnel driving. *Bull Int Assoc Eng Geol* 2(1):39–56
- Ii H, Kagami H (1997) Groundwater level and chemistry changes resulting from tunnel construction near Matsumoto City, Japan. *Environ Geol* 31(1–2):76–84
- Käss W (1998) Tracing technique in geohydrology. Balkema, Rotterdam, 600 pp
- Keller B (1992) Hydrology of the Swiss Molasse basin: a review of current knowledge and considerations for the future. *Eclogae Geol Helv* 85(3):611–652
- Kitterod NO, Colleuille H, Wong WK, Pedersen TS (2000) Simulation of groundwater drainage into a tunnel in fractured rock and numerical analysis of leakage remediation, Romeriksporten tunnel, Norway. *Hydrogeol J* 8(5):480–493
- Kolymbas D, Wagner P (2007) Groundwater ingress to tunnels: the exact analytical solution. *Tunn Undergr Space Technol* 22(1):23–27
- Kreft A, Zuber A (1978) Physical meaning of dispersion equation and its solution for different initial and boundary conditions. *Chem Eng Sci* 33(11):1471–1480
- Kvaerner J, Klove B (2006) Tracing sources of summer streamflow in boreal headwaters using isotopic signatures and water geochemical components. *J Hydrol* 331(1–2):186–204
- Lee IM, Nam SW, Ahn JH (2003) Effect of seepage forces on tunnel face stability. *Can Geotech J* 40(2):342–350
- Marechal JC, Perrochet P (2003) New analytical solution for the study of hydraulic interaction between Alpine tunnels and groundwater. *Bull Soc Geol Fr* 174(5):441–448
- Molinero J, Samper J, Juanes R (2002) Numerical modeling of the transient hydrogeological response produced by tunnel construction in fractured bedrocks. *Eng Geol* 64(4):369–386
- Nunn JA, Hanor JS, Lee Y (2005) Migration pathways in the Central North Slope foreland basin, Alaska USA: solute and thermal constraints on fluid flow simulations. *Basin Res* 17(3):403–416
- Otz MH, Otz HK, Otz I, Siegel DI (2003) Surface water/groundwater interaction in the Piora Aquifer, Switzerland: evidence from dye tracing tests. *Hydrogeol J* 11(2):228–239
- Perrochet P (2005) Confined flow into a tunnel during progressive drilling: an analytical solution. *Ground Water* 43(6):943–946
- Perrochet P, Dematteis A (2007) Modeling transient discharge into a tunnel drilled in a heterogeneous formation. *Ground Water* 45(6):786–790
- Reznickova P, Paril P, Zahradkova S (2007) The ecological effect of drought on the macroinvertebrate fauna of a small intermittent stream: an example from the Czech Republic. *Int Rev Hydrobiol* 92(4–5):514–526
- Ricci Lucchi F (1986) The Oligocene to Recent foreland basins of the Northern Apennines. *Int Assoc Sedimento Spec Publ* 8:105–139
- Schnegg PA, Flynn R (2002) Online field fluorimeters for hydrogeological tracer tests. In: *Isotope und Tracer in der Wasserforschung*, vol 19. Technische Universität Bergakademie Freiberg, Germany, pp 29–36
- Sjolander-Lindqvist A (2005) Conflicting perspectives on water in a Swedish railway tunnel project. *Environ Values* 14(2):221–239
- Toride N, Leij FJ, van Genuchten MT (1993) A comprehensive set of analytical solutions for nonequilibrium solute transport with first-order decay and zero-order production. *Water Resour Res* 29(7):2167–2182
- Toride N, Leij FJ, van Genuchten MT (1999) The CXTFIT code for estimating transport parameters from laboratory or field tracer experiments. Research Report No. 137, US Salinity Laboratory, USDA, ARS, Riverside, CA
- Tseng DJ, Tsai BR, Chang LC (2001) A case study on ground treatment for a rock tunnel with high groundwater ingress in Taiwan. *Tunn Undergr Space Technol* 16(3):175–183
- Yang SY, Yeh HD (2007) A closed-form solution for a confined flow into a tunnel during progressive drilling in a multi-layer groundwater flow system. *Geophys Res Lett* 34(7):L07405
- Yoo CS (2005) Interaction between tunneling and groundwater: numerical investigation using three dimensional stress-pore pressure coupled analysis. *J Geotech Geoenviron Eng* 131(2):240–250
- Zattin M, Landuzzi A, Picotti V, Zuffa GG (2000) Discriminating between tectonic and sedimentary burial in a fore deep succession, Northern Apennines. *J Geol Soc Lond* 157:629–633